International Journal of Medical Physics, Clinical Engineering and Radiation Oncology, 2025, 14(3), 100-111
https://www.scirp.org/journal/ijmpcero
ISSN Online: 2168-5444
ISSN Print: 2168-5436

Performance Analysis and Cross-Calibration of PPC-40 and FC65-P Ionization Chambers in Low-Energy Electron Beams Absolute Dosimetry

Abdul Momin, Motiur Rahman, Fajle Rabby, Rubel Ahmed, Ayesha Siddika Borna, AKM Ahsan Habib

Department of Oncology, TMSS Cancer Center, Bogura, Bangladesh
Email: tmss.tcc@gmail.com, motiur.delta@gmail.com

How to cite this paper: Momin, A., Rahman, M., Rabby, F., Ahmed, R., Borna, A.S. and Habib, AKM.A. (2025) Performance Analysis and Cross-Calibration of PPC-40 and FC65-P Ionization Chambers in Low-Energy Electron Beams Absolute Dosimetry. *International Journal of Medical Physics, Clinical Engineering and Radiation Oncology*, **14**, 100-111.
https://doi.org/10.4236/ijmpcero.2025.143008

Received: May 26, 2025
Accepted: July 18, 2025
Published: July 21, 2025

Abstract

Algorithm of electron beam dose delivery is dissimilar in comparison to X-ray radiation therapy. Therefore, absolute dosimetry of low energy like (≤9 MeV) is fundamentally effective in electron beam radiation therapy by a linear accelerator. This effectively needs evaluation of cross calibration by PPC-40 and FC65-P ionization chambers for accurate dosimetry to assure quality of treatment with clinical accuracy. Implications of results enunciated in this paper show that salient features are documented. The FC65-P chamber exhibited a deviation of up to 1.04% at shallow depths, indicating limitations for low-energy electron beams. In contrast, the PPC-40 demonstrated superior accuracy in surface dose and shallow-depth measurements due to its parallel-plate design and larger effective volume. The importance of cross-calibration yielded a new correction factor of 1.01, allowing conversion of FC65-P dose measurements to PPC-40 values. This relationship remained stable under controlled conditions. The clinical significance of the selection of ionization chamber for low energy electrons dosimetry is absolutely required for treatment precision and patient safety in electron beam radiation therapy (EBRT).

Keywords

LINAC, Low-Energy Electron Beams, Ionization Chambers, Cross-Calibration and Absolute Dosimetry, PDD, EBRT, PPC-40, FC65-P

1. Introduction

Cancer treatment relies on three primary modalities: external beam radiation

therapy (EBRT), chemotherapy, and surgery. Depending on the disease stage and clinical requirements, a combination of these modalities is often employed for optimal management. Among them, EBRT remains a cornerstone of modern cancer therapy, with over 50% of cancer patients worldwide receiving radiation treatment at some stage [1] [2]. EBRT primarily utilizes megavoltage electron beams (6 - 22 MeV) or X-ray photons (4 - 25 MV) from linear accelerators (LINACs), as well as γ-ray photons from teletherapy machines [3]. Unlike megavoltage photon beams, electron beams exhibit a high surface dose with rapid dose fall-off, making them particularly effective for treating superficial tumors (≤5 cm depth). Their finite penetration depth distinguishes them from photons, allowing precise dose delivery to target tissues while minimizing exposure to underlying healthy structures [4].

Electron beams are generated by LINACs, where their energy levels (typically 4 - 25 MeV) can be tailored to match tumor depth and clinical requirements. Their key advantage lies in their ability to deposit maximum energy near the surface and rapidly attenuate beyond the target, reducing toxicity to deeper tissues such as the heart, lungs, and bones. This is particularly advantageous in head and neck, breast, and skin cancer treatments, where minimizing collateral damage is crucial in improving patient outcomes [5].

To optimize electron beam therapy, various clinical strategies are employed. Bolus materials, made of tissue-equivalent substances, are often placed on the skin surface to fine-tune dose distribution, ensuring precise coverage of superficial tumors.

Patient treatment accuracy depends on the quality assurance of ionization chambers and prescribed dose, and about 90% of dose lines for electron beam. Besides, parameters like beam energy, field size, treatment dose, and prescribed dose [6].

2. Objective

This study aims to evaluate the performance and cross-calibration of PPC-40 and FC65-P ionization chambers in low-energy electron beam dosimetry to enhance clinical accuracy. Also comparing the sensitivity of the PPC-40 and FC65-P ion chambers to changes in beam parameters such as energy, field size, and dose rate, investigating how each ion chamber responds to different qualities of electron beam.

Dosimetry involves the measurement and calibration of the dose delivered by an electron beam, typically used in treating superficial tumors. Ionization chambers are the most common instruments used for absolute dosimetry. Here, we have used plane parallel (PPC-40) and cylindrical (FC65-P) ionization chamber to measure the ionization produced by the electron beam. Dosimetry is performed under standardized reference conditions, including 10×10 cm^2 field size, source-to-surface distance (SSD) at 100 cm, and depth in water phantom at 1.27 cm and

2 cm corresponding to 6 MeV and 9 MeV energy to ensure consistency and comparability. Ionization chambers are calibrated in a standard laboratory using a known radiation source. The calibration factor is then used to convert the measured ionization to absorbed dose. Protocols like IAEA TRS-398 and AAPM TG-51 provide guidelines for performing absolute dosimetry in clinical settings. These protocols standardize procedures for measuring and calculating the absorbed dose, accounting for factors like beam quality, energy, and ionization chamber type. Corrections are applied for factors like ion recombination, polarity effects, temperature and pressure, ensuring the accuracy of the dose measurements.

3. Materials and Methods

The dosimetric equipment was deployed under the exposure arrangement of the LINAC machine to verify electron beams characteristics [7]. The analysis of the dosimetric parameters was performed by using MyQA Accept software. The main intention of this process is to substantiate the measured dosimetric characteristics of a LINAC machine in terms of standard protocols.

3.1. Ionization Chamber Setup

According to IAEA "TRS 398" protocol for $R_{50} < 4$ gm/cm^2 phantom material will water or plastic. Finally, assured that the phantom is stable and won't move during measurements. The ionization chamber was inserted into the water phantom holder and ensured the chamber is aligned perpendicular to the beam direction. Laser and marker were used to verify the chamber's positioned and stably within the water phantom. For plane parallel chamber the reference point is on the inner surface of the window at its center and for cylindrical chamber the reference point on the central axis at the center of the cavity.

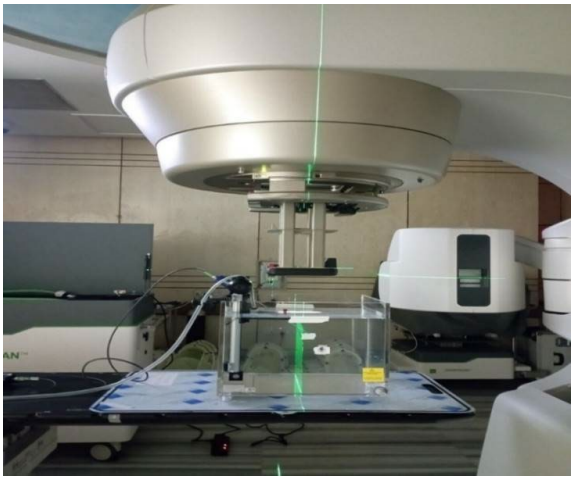

Figure 1. One Dimensional (1D) phantom setup.

Based on the data presented in **Figure 6** and **Figure 7**, the half-value depths (R_{50}) (in **Table 2**) for 6 MeV and 9 MeV electron energies were determined. These

values were then substituted into Equation (2) to calculate the reference depths (z_{ref}), resulting in values of 1.27 cm for 6 MeV and 2.00 cm for 9 MeV. Subsequently, both the PPC-40 (plane-parallel) and FC65-P (cylindrical) ionization chambers were placed in the water phantom at their respective reference depths. Then the PPC-40 and FC65-P ionization chambers were connected to the electrometer and applying bias voltage for ion collection. In accordance with the "TRS-398" protocol, bias voltages of **+300 V**, **−300 V**, and **+150 V** were applied during the measurements. For each bias voltage setting, **three sets of data** were recorded to ensure consistency and reliability of the readings (Figures 1-3).

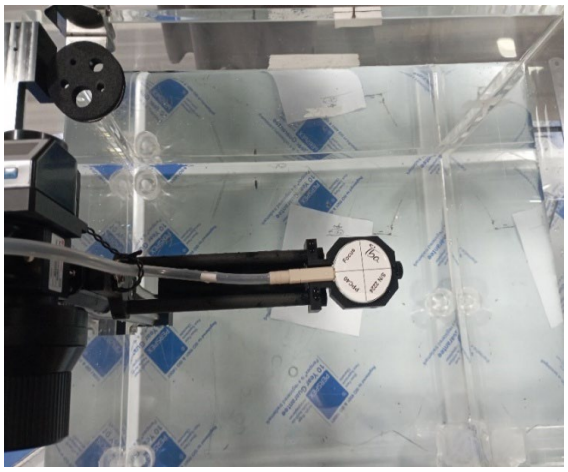

Figure 2. Experimental setup of plane parallel ionization chamber.

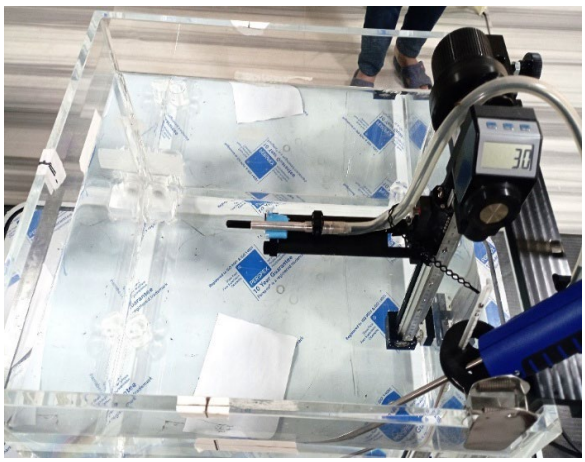

Figure 3. Experimental setup of cylindrical ionization chamber.

3.2. Measurement of Beam Quality

The beam quality index for electron beams is the half-value depth in water R_{50}. This is the depth in water (g/cm^2) at which the absorbed dose is 50% of its value at the absorbed dose maximum, measured with a constant SSD of 100 cm and a field size at the phantom surface of at least 10 cm × 10 cm for $R_{50} < 7$ g/cm^2 ($E_0 \leq$ 16 MeV) [8]. From relative ionization data we have got the value of $R_{50,\,ion}$ and

then the reference conditions for the determination of R_{50} are given below for electron beam qualities [9],

$$R_{50} = 1.029 R_{50,ion} - 0.06\, g/cm^2 \left(R_{50,ion} \le 10\, g/cm^2 \right) \quad (1)$$

3.3. Reference Conditions

To determine the value from equation (1) and from absorbed dose versus depth curve we have got the value of R_{50} and the reference depth z_{ref} is [10].

$$z_{ref} = 0.6\, R_{50} - 0.1\ g/cm^2 \left(R_{50} in\, g/cm^2 \right) \quad (2)$$

This depth is close to the depth of the absorbed-dose maximum z_{max} at beam qualities $R_{50} < 4$ g/cm^2 ($E_o \le 10$ MeV), but at higher beam qualities is deeper than z_{max}.

3.4. Pressure and Temperature Correction Factors

As all chambers recommended in TRS 398 are open to the ambient air, the mass of air in the cavity volume is subject to atmospheric variations. The correction factor:

$$\mathrm{KTP} = \frac{(273.2 + T) P_0}{(273.2 + T_0) P} \quad (3)$$

Should be utilized to convert the mass of air in the cavity to reference conditions. Here, P and T represent the cavity air pressure and temperature during the measurements, while P_o and T_o denote the reference values (typically 1013.25 hPa and 20˚C) [9].

3.5. Polarity Effect

Polarity effect can be particularly significant in charged particle beams, especially electrons. The influence of using polarizing potentials of opposite polarity for each user beam quality Q can be accounted for by applying a correction factor:

$$k_{pol} = \frac{|M_+| + |M_-|}{2M} \quad (4)$$

where, M_+ and M_- are the electrometer readings obtained at positive and negative polarity, respectively, and M is the electrometer reading obtained with the polarity used routinely [9].

3.6. Ion Recombination Correction (Two Voltage Method)

The incomplete collection of charge in an ionization chamber cavity due to the recombination of ions necessitates the application of a correction factor (k_s). For pulsed beams, "TRS 398" deriving the correction factor (k_s) using the two-voltage method [11]. This method assumes a linear relationship between 1/M and 1/V, utilizing the measured values of collected charges M_1 and M_2 at polarizing voltages V_1 and V_2, respectively, under the same irradiation conditions. Here, V_1 represents the normal operating voltage, while V_2 is a lower voltage; ideally, the ratio V_1/V_2 should be equal to 2 or greater than 3. The recombination correction factor k_s at

the normal operating voltage V_1 is obtained from

$$k_s = a_0 + a_1\left(\frac{M_1}{M_2}\right) + a_2\left(\frac{M_1}{M_2}\right)\times\left(\frac{M_1}{M_2}\right) \tag{5}$$

where, the constants a_i are given for pulsed scan radiation (Table 1).

Table 1. Constants a_0, a_1, and a_2 used in the two-voltage method for calculating the ion recombination correction factor k_s in pulsed radiation, based on a voltage ratio $V_1/V_2 = 2.0$.

The voltage ratio, $\frac{V_1}{V_2}$	Pulsed radiation		
	a_0	a_1	
2.0	2.337	−3.636	2.999

The correction factor k_s evaluated using the two voltages method in pulsed beams corrects for both general and initial recombination [9] [12].

3.7. Corrected Dosimeter Reading

Corrected dosimeter reading at the voltage V_1:

$$M_Q = M_1.h_{pl}.k_{TP}.k_{ele}.k_{pol}.k_s \tag{6}$$

In our experiment we used a water phantom so the fluence scaling factor, $h_{pl} = 1$. The electrometer is not calibrated separately so the value of electrometer calibration factor, $k_{ele} = 1$ [9].

3.8. Absorbed Dose at z_{max}

Clinical normalization most often takes place at the depth of the dose maximum z_{max} which, in the present Code of Practice, does not always coincide with z_{ref}. To determine the absorbed dose to water at the depth of dose maximum z_{max}: [9] [13]

$$D_{w,Q}\left(z_{\max}\right) = \frac{100D_{w,Q}\left(z_{ref}\right)}{PDD\left(z_{ref}\right)} \tag{7}$$

3.9. Cross-Calibration

Cross-calibration of an ionization chamber is the process of comparing the response of a field or clinical chamber to that of a well-characterized reference chamber under identical radiation beam conditions. The ratio of their readings is used to derive a calibration coefficient for the field chamber, ensuring its dose measurements remain traceable and accurate. The calibration factor

$$N_F = \frac{M_R}{M_F} \tag{8}$$

N_F = Calibration factor of the field chamber in the electron beam;
M_R = Dose measured by the reference chamber (PPC-40);
M_F = Charge (or dose) measured by the field chamber (FC65-P).

3.10. Sources of Systematic Errors

There are several potential sources of error in dosimetric measurements. A common issue arises from the improper recording of ambient conditions, such as temperature and pressure, which must be measured with precision and consistency. The majority of errors typically occur during the setup of the ionization chamber, including its positioning and alignment. Furthermore, inaccuracies can be introduced during ion collection by the electrometer and throughout the dose calculation process. These errors can be minimized by ensuring meticulous chamber setup, verifying the accuracy and calibration of the thermometer, barometer, and electrometer, and maintaining the correct bias voltage throughout the measurement procedure.

4. Results

After obtaining the PDD curves, the ionization data were converted into dose curves to ensure accurate dose measurement and meet the requirements of dosimetry protocols. PDD curves offer a visual representation of relative ionization, but dose curves derived from chamber measurements are essential for precise calibration and treatment accuracy. Using equation (2) from the TRS-398 protocol, the values of R_{50} and the reference depths z_{ref} were calculated for both 6 MeV and 9 MeV electron energies.

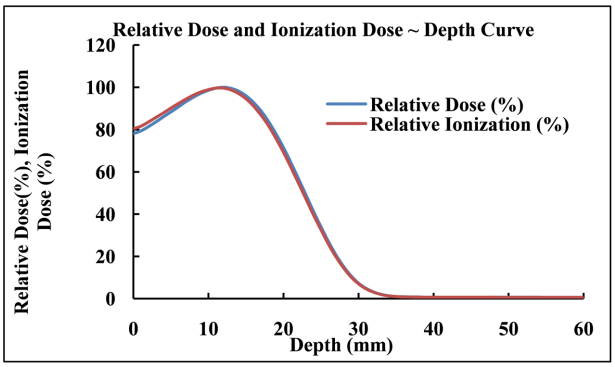

Figure 4. Relative and ionization doses versus depth curve for 6 MeV energy.

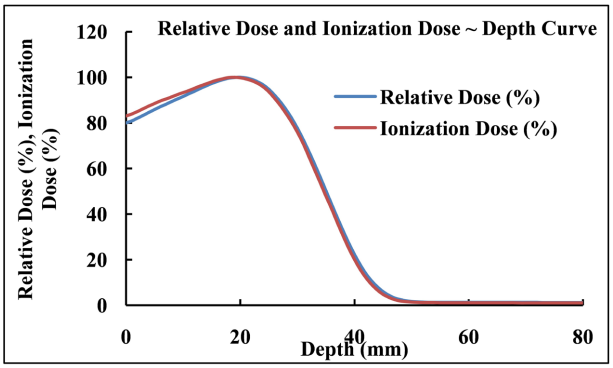

Figure 5. Relative dose and Ionization dose versus depth curve for 9 MeV energy.

PDD curves are shown in Figure 4 and Figure 5. From the dose curves, R_{50} values were found for 6 MeV and 9 MeV beams which are presented in Figure 6 and Figure 7.

Following cross-calibration, Table 4 demonstrates the improved agreement between PPC-40 and FC65-P chambers, with dose readings showing near equivalence across all sessions and energies. This confirms the effectiveness of the cross-calibration process and the suitability of FC65-P as a substitute when PPC-40 is unavailable for low-energy electron dosimetry.

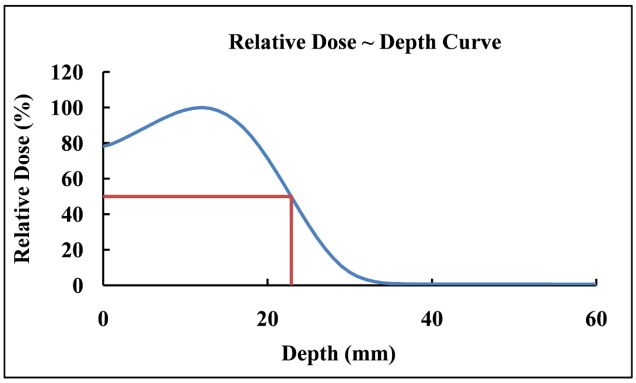

Figure 6. R50 value curve for 6 MeV energy.

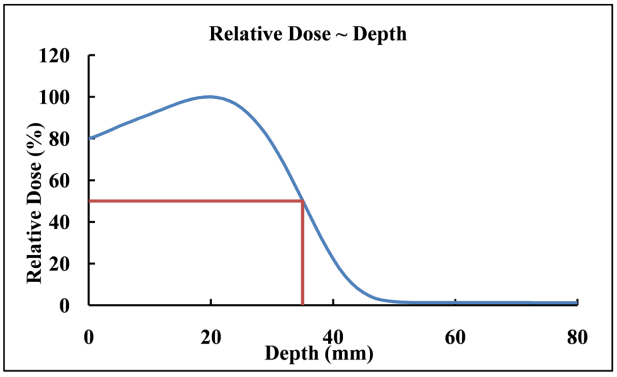

Figure 7. R50 value curve for 9 MeV energy.

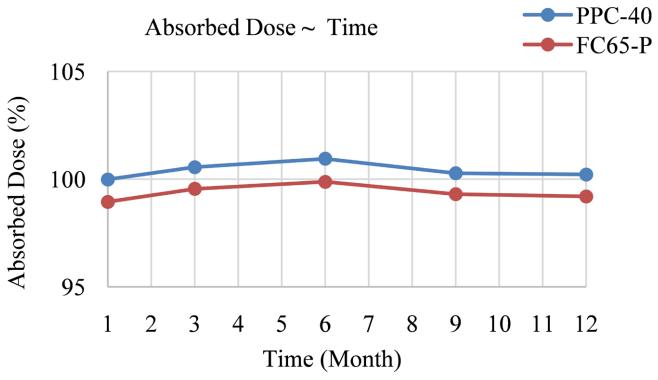

Figure 8. Graph before calibration for 6 MeV energy.

Table 2. The half-value depth, reference depth and PDD obtained from depth dose curves (**Figure 4** and **Figure 5**). The K_Q. values are evaluated by interpolating the calculated values and reference table from TRS 398.

Energy (MeV)	0 (cm)	z_{ref} (cm)	PDD at zref (%)	K_Q value using	
				PPC-40 Ion-chamber	FC65-P Ion-chamber
6	2.29	1.27	99.90	0.943	0.920
9	3.50	2.00	99.95	0.925	0.916

Table 3. Absorbed dose data at z_{max}, before the cross-calibration of PPC-40 and FC65-P ionization chamber for 6 MeV & 9 MeV energy.

Energy	Session	Absorbed Dose at z_{max} (cGy)		% Deviation	Cross-Calibration Factor for FC65-P
		PPC-40	FC65-P		
6 MeV	January	99.99	98.95	1.04	1.01
	March	100.56	99.55	1.00	1.01
	June	100.90	99.88	1.01	1.01
	September	100.28	99.31	0.97	1.01
	December	100.22	99.20	1.02	1.01
9 MeV	January	100.98	99.95	1.02	1.01
	March	100.95	99.98	0.96	1.01
	June	100.17	99.20	0.97	1.01
	September	99.93	98.90	1.03	1.01
	December	100.10	99.08	1.02	1.01

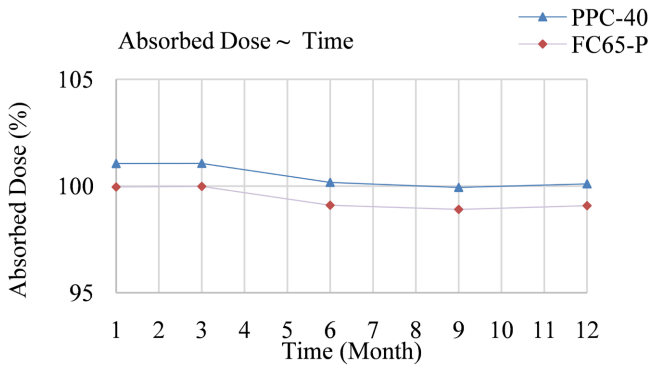

Figure 9. Graph before calibration for 9 MeV Energy.

Table 2 presents the calculated R_{50}, reference depths, and PDD at z_{ref}, along with the corresponding k_Q values for both PPC-40 and FC65-P ionization chambers.

Using equation (8), we got the calibration factors for all sessions. **Table 3** summarizes the absorbed dose measurements at z_{max} before cross-calibration. The deviation in dose readings between PPC-40 and FC65-P chambers ranged from 0.97% to 1.04%, indicating a measurable difference in chamber response over time and energy. **Figure 8** and **Figure 9** depict these pre-calibration comparisons

graphically for 6 MeV and 9 MeV energies, respectively.

Figure 10 and Figure 11 show the graphical representation after calibration for the 6 MeV and 9 MeV electron energies. Table 4 presents the data after calibration.

The averaged calibration factor, $N_{F,avg}$ **= 1.01** which is the new calibration factor for FC65-P ionization chamber.

Table 4. Absorbed dose data at z_{max}, after the cross-calibration of PPC-40 and FC65-P ionization chamber for 6 MeV & 9 MeV energy.

Energy	Session	Absorbed Dose at z_{max} (cGy) after cross-calibration	
		PPC-40	FC65-P
6 MeV	January	99.99	99.94
	March	100.56	100.54
	June	100.90	100.88
	September	100.28	100.30
	December	100.22	100.19
9 MeV	January	100.98	100.94
	March	100.95	100.98
	June	100.17	100.19
	September	99.93	99.88
	December	100.10	100.07

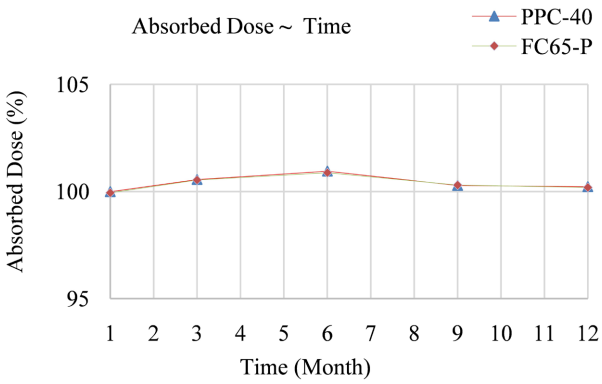

Figure 10. Graph after calibration for 6 MeV energy.

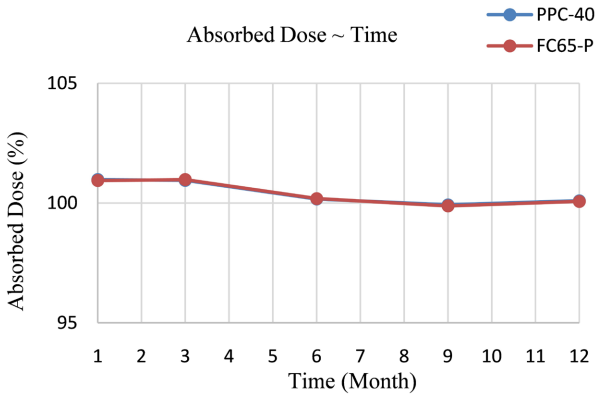

Figure 11. Graph after calibration for 6 MeV energy.

5. Discussion

This study of evaluating PPC-40 and FC65-P ionization chamber's accuracy, consistency, cross calibration and practical applicability was done for clinical electron beam dosimetry. In dosimetry, temperature and pressure are the most important factors and these variations directly affect the ionization efficiency of the PPC-40 and FC65-P chambers. So, it is measured carefully and cross checked to perform the dosimetry.

At lower energies (6 MeV and 9 MeV), the PPC-40 is more reliable, reflecting its design advantages for measuring lower-energy electron beams, where dose gradients are steeper. The response of the FC65-P at lower energies is observed to be less consistent, showing a slight under-response compared to the PPC-40. This under-response can be attributed to the larger sensitive volume of the cylindrical chamber, which leads to dose averaging effects that are less pronounced in parallel-plate chambers like the PPC-40. The findings of this study provide critical insights into the dosimetric characteristics of these chambers and their potential suitability for clinical use during radiation therapy. From a clinical perspective, this study helps determine whether the LINAC machine is delivering a dose lower or higher than the prescribed dose to the patient.

6. Conclusion

Result of experimentation suggests that for electron beam energies at 6 MeV and 9 MeV, both the plane-parallel and cylindrical ionization chambers can be used interchangeably for dosimetry. This is particularly relevant for quality assurance purposes, where a plane-parallel chamber might not be available. In such cases, a cylindrical ionization chamber can serve as a suitable alternative. The result of our study indicates that the maximum dose difference between the PPC-40 and FC65-P ionization chambers was within 1.04%. According to "TRS 398", a difference within this limit is considered acceptable, confirming the reliability of both chambers for low-energy electron beam dosimetry. After the cross calibration it was seen that both chambers give the same absorbed dose value. Finally, we can say that in which cancer center PPC-40 ionization chamber is not available they can use FC65-P ionization chamber to perform their electron beam absolute dose calibration for 6 MeV and 9 MeV energy using our measured calibration factor 1.01.

Acknowledgements

We sincerely acknowledge the invaluable support of Prof. Dr. Hosne Ara Begum, Executive Director (ED), and Rtn. Dr. Md. Matiur Rahman, Deputy Executive Director-2 (DED-2) of TMSS. Their constant encouragement and leadership were instrumental in conducting this research at TMSS Cancer Center. We remain grateful for the facilities and motivation they provided throughout the study.

Conflicts of Interest

The authors declare no conflicts of interest regarding the publication of this paper.

References

[1] Connell, P.P. and Hellman, S. (2009) Advances in Radiotherapy and Implications for the Next Century: A Historical Perspective. *Cancer Research*, **69**, 383-392. https://doi.org/10.1158/0008-5472.can-07-6871

[2] Ferlay, J., Soerjomataram, I., Ervik, M., Dikshit, R., Eser, S., Mathers, C., *et al.* (2013) GLO-BOCAN 2012: Estimated Cancer Incidence, Mortality, and Prevalence Worldwide in 2012 v1.0: IARC Cancer Base No. 11. IARC Publications.

[3] Ding, G.X. (2004) An Investigation of Accelerator Head Scatter and Output Factor in Air. *Medical Physics*, **31**, 2527-2533. https://doi.org/10.1118/1.1784131

[4] Baskar, R., Lee, K.A., Yeo, R. and Yeoh, K. (2012) Cancer and Radiation Therapy: Current Advances and Future Directions. *International Journal of Medical Sciences*, **9**, 193-199. https://doi.org/10.7150/ijms.3635

[5] Hogstrom, K.R. and Almond, P.R. (2006) Review of Electron Beam Therapy Physics. *Physics in Medicine and Biology*, **51**, R455-R489. https://doi.org/10.1088/0031-9155/51/13/r25

[6] Su, Z., Indelicato, D.J., Mailhot, R.B. and Bradley, J.A. (2020) Impact of Different Treatment Techniques for Pediatric Ewing Sarcoma of the Chest Wall: IMRT, 3DCPT, and IMPT with/without Beam Aperture. *Journal of Applied Clinical Medical Physics*, **21**, 100-107. https://doi.org/10.1002/acm2.12870

[7] Rahman, M., Shamsuzzaman, M., Sarker, M., Jobber, A., Mia, M., Bairagi, A.K., *et al.* (2021) Dosimetric Characterization of Medical Linear Accelerator Photon and Electron Beams for the Treatment Accuracy of Cancer Patients. *World Journal of Advanced Engineering Technology and Sciences*, **3**, 41-59. https://doi.org/10.30574/wjaets.2021.3.1.0046

[8] IAEA International Atomic Energy Agency (1997) The Use of Plane-Parallel Ionization Chambers in High-Energy Electron and Photon Beams: An International Code of Practice for Dosimetry. Technical Report Series No. 381, IAEA.

[9] International Atomic Energy Agency (2024) Absorbed Dose Determination in External Beam Radiotherapy: An International Code of Practice for Dosimetry Based on Standards of Absorbed Dose to Water, Technical Reports Series No. 398 rev1. IAEA.

[10] Burns, D.T., Ding, G.X. and Rogers, D.W.O. (1996) R_{50} as a Beam Quality Specifier for Selecting Stopping-Power Ratios and Reference Depths for Electron Dosimetry. *Medical Physics*, **23**, 383-388. https://doi.org/10.1118/1.597893

[11] Boag, J.W. and Currant, J. (1980) Current Collection and Ionic Recombination in Small Cylindrical Ionization Chambers Exposed to Pulsed Radiation. *The British Journal of Radiology*, **53**, 471-478. https://doi.org/10.1259/0007-1285-53-629-471

[12] Derikum, K. and Roos, M. (1993) Measurement of Saturation Correction Factors of Thimble-Type Ionization Chambers in Pulsed Photon Beams. *Physics in Medicine and Biology*, **38**, 755-763. https://doi.org/10.1088/0031-9155/38/6/009

[13] Chowdhury, M.R.I., Rabby, M.F., Ahmed, R., Akter, M. and Rahman, M.M. (2024) A Comparative Study of Photon Beam Percentage Depth Dose of a Recently Installed Varian Vitalbeam Linear Accelerator at TMSS Cancer Center, Bangladesh. *International Journal of Radiology & Radiation Therapy*, **11**, 100-104. https://doi.org/10.15406/ijrrt.2024.11.00394